EXPERIMENTAL RESEARCH OF AERODYNAMIC PERFORMANCE OF MIL-171A2 HELICOPTER AIRFRAME VARIABLE MODEL IN T-1 WIND-TUNNEL OF MAI

B.L. Artamonov

Moscow Aviation Institute, Moscow, Russia, k102@mai.ru

V.A. Ivchin

JSC “Moscow Helicopter Plant n.a. M.L. Mil”, Tomilino, Moscow Region, Russia, Vivtchin@mi-helicopter.ru

The paper describes design and manufacturing technology of variable wind-tunnel model of Mil-171A2 single-rotor helicopter airframe. This model was created for experimental optimization of helicopter aerodynamic configuration by varying the shape of its nose and tail parts, external fuel tanks, horizontal stabilizer, tail rotor pylon and engine air particle separators. The variable wind-tunnel model was designed on the basis of the 3-D model of helicopter airframe surface. This 3-D model was created with the use of the Solid Works geometric computer simulation system. The variable wind-tunnel model was manufactured with the use of 3-D prototyping technology on a computer numerical control machine.

The experimental research of aerodynamic performance of the wind-tunnel model was performed in T-1 wind-tunnel of MAI for the following conditions: range of the angles of attack from -30 to +30 degrees; range of yaw angles from -180 to +180 degrees; different setting angles of horizontal stabilizer and vertical fin. The paper lists comparative aerodynamic performance of the different configurations of the wind-tunnel model. The assessment of the impact of the variable model parts on the aerodynamic forces and moments, which emerge and act on the helicopter airframe in different flight modes, is given.

Mil-171A2 helicopter is the heavily modernized version of Mil-17 helicopter, which is developed on the basis of Mil-171A1 helicopter (Fig. 1). Mil-171A1 helicopter is manufactured by Ulan-Ude Aircraft Plant. It has been certified for commercial operation by AR MAK (Aviation Register of Interstate Aviation Committee). The main modernization concept consists in improving the operating performance of this helicopter while staying within the same cur-rent market niche [11]. This helicopter will have the sling capacity of up to 5 tons. It will be able to fly in all climatic regions at the air temperatures of -50…+50 degrees at the higher allowable speeds of the side wind [9]. The flight range with main fuel tanks will be increased up to 850 km. The cruise speed will be increased as well. The yaw stability will be improved. The mock-up model of Mil-171A2 helicopter (Fig. 2) was shown on HeliExpo-2012 Helicopter Exhibition in Dallas, USA, in February of 2012 [13].

Fig. 1. Mil-171A1 helicopter

Fig. 2. Mock-up model of Mil-171A2 helicopter

To achieve the declared flight performance MVZ (Moscow Helicopter Plant n.a. M.L. Mil) has planned to carry out the experimental investigation of optimization of the aerodynamic configuration of the modernized helicopter. The experimental investigation provided for the research of the different con-figurations of the model of Mil-171A2 helicopter airframe in T-1 wind-tunnel of MAI for the range of the angles of attack and yaw, which would cover all flight modes. It also included drawing up the recommendations for improvement of airframe shape optimization based on the results of the visualization of the air flow near the model surface.

A state of the art type wind-tunnel model is created as a scaled-down copy of aircraft with the same external shape, which is manufactured with high precision and quality. In fact, the high manpower effort that is required for design and manufacturing of wind-tunnel models results in long terms of their creation (up to one year). Such long development terms are unacceptable under the conditions of stiff competition, which has emerged in aviation industry. Therefore the reduction of terms, and manpower effort required for design and manufacturing of wind tunnel models becomes an important factor, especially when timing and financial resources are limited. The experience, which was accumulated at TsAGI n.a. N.E. Zhukovsky, demonstrates that the most important way of reducing the terms and manpower effort required for wind-tunnel model creation is the complete integrated automation of all elements of this process (design, structure design, production design, manufacturing, instrumental monitoring) on the basis of usage of the modern information technologies [4].

The wind-tunnel model of Mil-171A2 helicopter was designed on the basis of the initial data from the full-scale 3-D models of surfaces of the base and varied elements of the helicopter airframe, which was created at the Moscow Helicopter Plant (MVZ) n.a. M.L. Mil by using the Solid Works 3D mechanical CAD system (Fig. 3). The notation conventions of the varied elements of wind-tunnel helicopter model are designated in Table 1.

Base airframe elements

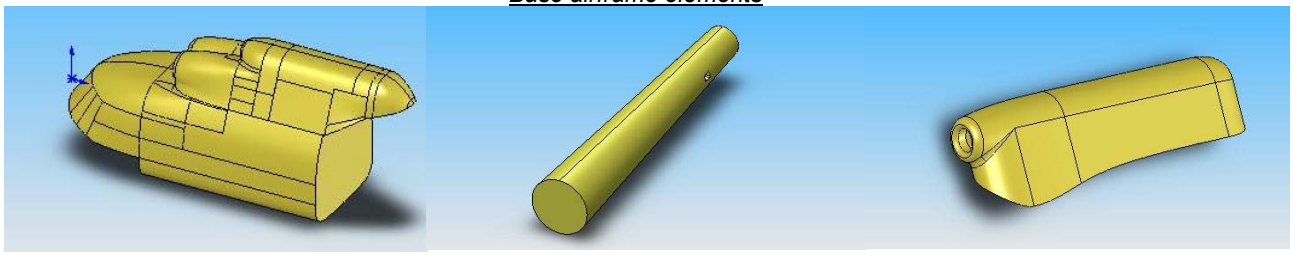

a) central part of fuselage | b) tail boom | c) kerosene-combustion heater *KO-50*

Variants of nose parts of fuselage

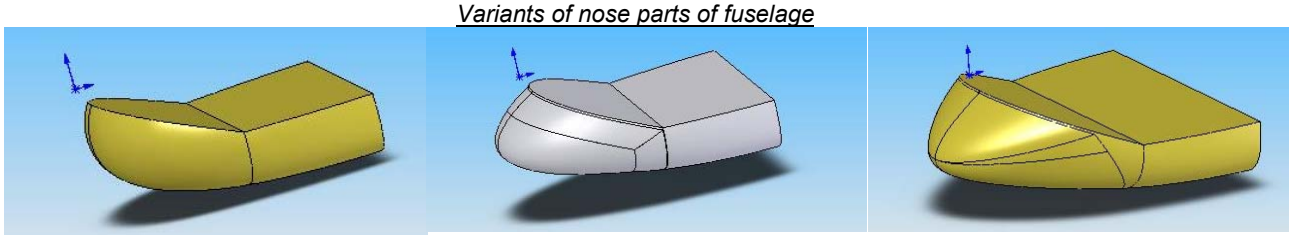

a) nose of serially produced *Mil-17* | b) "dolphin nose" of *Mil-171A2* | c) "narrow nose" of *Mil-171A2* with the radar

Variants of tail parts of fuselage

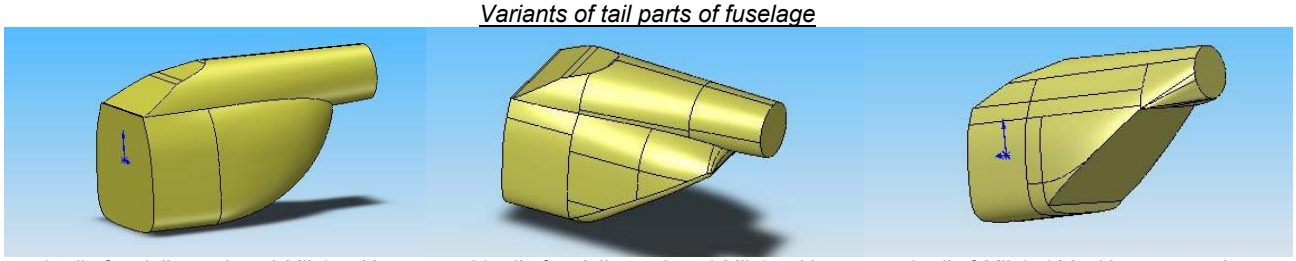

a) tail of serially produced *Mil-17* with standard cargo doors | b) tail of serially produced *Mil-17* with standard cargo ramp | c) tail of *Mil-171A2* without cargo doors and cargo ramp

Variants of fuel tanks

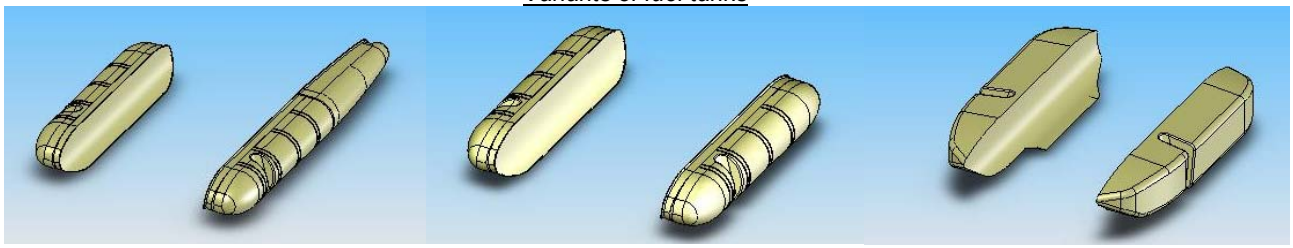

a) fuel tanks of serially produced *Mil-17* with *KO-50* kerosene-combustion heater | b) typical fuel tanks of *Mil-171A2* without *KO-50* kerosene-combustion heater | c) fuel tanks of *Mil-171A2* with increased capacity

Variants of tail rotor pylon | Variants of horizontal stabilizer | Variants of engine air particle separator

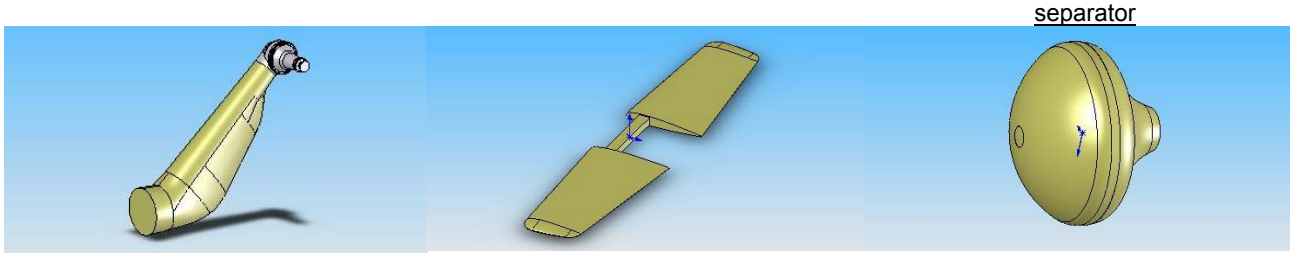

a) tail rotor pylon of serially produced I *Mil-17* | a) horizontal stabilizer of serially produced *Mil-17* | a) engine air particle separator of "mushroom" type of *Mil-17*

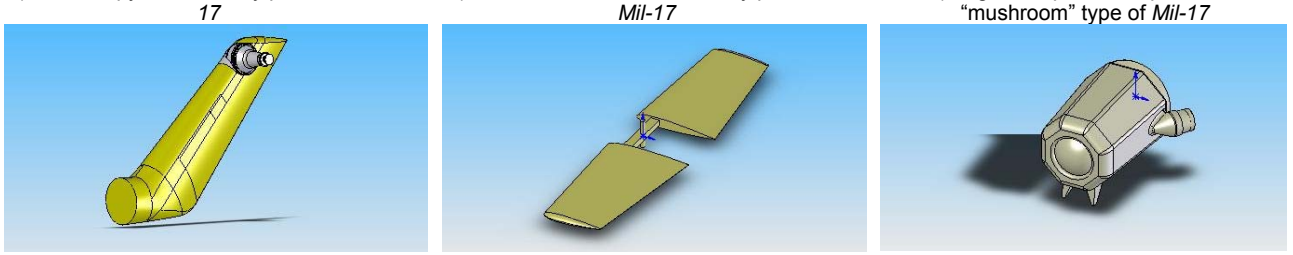

b) tail rotor pylon of *Mil-171A2* with increased surface area of vertical fin | b) horizontal stabilizer of *Mil-171A2* with increased surface area | b) engine air particle separator of PAL pyramid type for *Mil-171A2*

Fig. 3. *3D*–models of surfaces of base and variable elements of helicopter airframe

T a b l e 1

Notation conventions of variable airframe elements of helicopter model

Item number in sequence	Notation symbol	Description of variable structure element of wind-tunnel model
		Nose parts of fuselage
1.	NPF1 -	nose of serially produced *Mil-17*,
2.	NPF2 -	"dolphin nose" of *Mil-171A2*,
3.	NPF3 -	"narrow nose" of *Mil-171A2* with the radar
		Tail parts of fuselage
1.	TPF1 -	tail of serially produced *Mil-17* with standard cargo doors,
2.	TPF2 -	tail of serially produced *Mil-17* with standard cargo ramp,
3.	TPF3 -	tail of passenger version of *Mil-171A2* with fairing (with new cargo doors),
4.	TPF4 -	tail of the stretched version of *Mil-171A2* with closed cargo ramp of the new type,
5.	TPF5 -	tail of the stretched version of *Mil-171A2* with open cargo ramp of the new type.
		Tail rotor pylon
1.	TRP1 -	tail rotor pylon of serially produced *Mil-17*,
2.	TRP2 -	tail rotor pylon of *Mil-171A2* with increased surface area of vertical fin and discretely varied angle between the plane of the vertical fin and the fore-and-aft plane of symmetry of the helicopter (the setting angle of the vertical fin).
		Horizontal stabilizers
1.	HS1 -	horizontal stabilizer of serially produced *Mil-17*,
2.	HS2 -	horizontal stabilizer of *Mil-171A2* with increased surface area,
3.	HS3 -	*H*-shaped horizontal stabilizer of *Mil-171A2* with increased surface area and two vertical fins.
		Fuel tanks
1.	FT1 -	fuel tanks of serially produced *Mil-17* with *KO-50* kerosene-combustion heater,
2.	FT2 -	typical fuel tanks of *Mil-171A2* without *KO-50* kerosene-combustion heater,
3.	FT3 -	fuel tanks of *Mil-171A2* with increased capacity.
		Engine air particle separators
1.	EAPS1 -	engine air particle separator of "mushroom" type of *Mil-17*,
2.	EAPS2 -	engine air particle separator of *PAL* pyramid type for *Mil-171A2*.
		System of heating and ventilation of the cabin
1.	KCH -	*KO-50* kerosene-combustion heater.

The variable wind-tunnel model has been created on a scale of 1:20. This model is a the detachable structure (Fig. 4), which consists of the unchanged central part of fuselage and variable nose and tail parts of fuselage, tail rotor pylon, horizontal stabilizer, external fuel tanks, engine air particle separators. The tail boom, the nose and main landing gear legs remained unchanged.

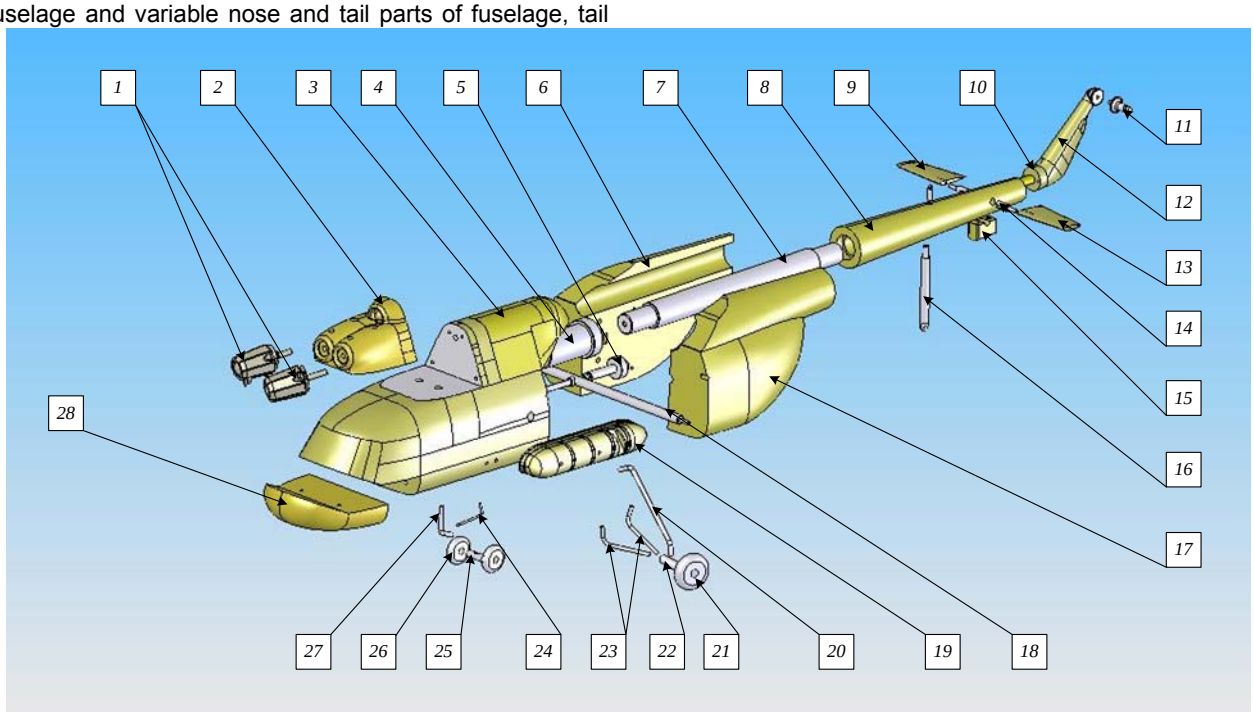

Fig. 4. Elements of *Mil-171A2* helicopter model structure

The metal bar (7) is attached to the central part of the fuselage (3) via the centring bushing (4). The tail boom (8) is screwed onto the metal bar (7). The tail rotor pylon (12) is attached to the tail boom (8) via the exchangeable spacer plates (10). The ability to replace and exchange the spacer plates (10) provides for discrete variation of the setting angle of the tail rotor pylon (12) (and of the setting angle of the vertical fin, respectively). The tail rotor gearbox (11) is attached via threaded fastening to the tail rotor pylon (12). The rotation axis (14) of the exchangeable horizontal stabilizer panels (9, 13) passes through the hole in the tail boom (8). The rotation axis (14) is fully fixed with the roll loading (15). Such attachment structure provides the variation of the setting angle of the horizontal stabilizer relative to the fuselage water line.

The exchangeable halves of the variable tail part of the fuselage (6, 17) are based on the cylindrical surface of the metal bar (7). These exchangeable halves of the variable tail part of the fuselage (6, 17) are fixed relative to the central fuselage part by the pins and are attached to each other by screws. The engines package (2) with the exchangeable engine air particle separators (1), variable fuel tanks (19) and nose parts of the fuselage (28) are centered by the pins and screwed to the central fuselage.

The nose landing gear leg consists of the following elements: two wheels (26), which are spindled on the axle (25); the shock strut (27) and the drag strut (24), which are fully fixed in the special holes of the central fuselage part (3). The right and left main landing gear legs have the same configuration and consist of the wheel axle (22), the horizontal struts (23) and the inclined shock strut (20), which are rigidly fixed in the special holes of the central fuselage part (3). The model is mounted on the *6KT1* six-component wind-tunnel balance with the help of the following: the horizontal bar (18), which passes through the hole in the central fuselage part (3) and is fixed with the mushroom-headed screw (5);–the vertical bar (16), which is screwed to the tail boom (8).

The variable wind-tunnel model of the helicopter was manufactured with the involvement of various *3-D* prototyping technologies [6, 7], which use the computer numerical control machines (Fig. 5): milling and lathe, laser sintering of metallic and non-metallic powders, laser stereo lithography processing. These machines are installed at the resource centers of MAI, which were created within the framework of the Program of development of MAI as the National Research University.

ProfiSpeed 600 Numerical Control milling machine

TPK-125A1-1 Numerical Control lathe machine

Viper si2TM laser stereo lithography processing machine

EOSINT M270 laser sintering machine

Zprinter 650 3D-Printer

Fig. 5. The computer numerical control machines, which were used for manufacturing the variable wind-tunnel model of Mil-171A2 helicopter

Various metallic and composite materials were used for manufacturing the wind-tunnel model elements. The list of these materials is adduced in Table 2. Four variants of the variable wind-tunnel model of helicopter are shown in Fig. 6. They were assembled from the different elements. Their notation conventions were designated according to the rules, which were established in the Table 1.

Table 2

Structure materials and machines, which were used for manufacturing the variable wind-tunnel model of Mil-171A2 helicopter

Structure elements of wind-tunnel model	Machines	Materials
Central part of fuselage, variable NPF, TPF, TRP and fuel tanks	*ProfiSpeed 600* Numerical Control milling machine	Oil-filled PA-6 polyamide (or caprolon B) of black color [*)]
Metal bar for TB attachment, centring bushing, horizontal bar, vertical bar	*TPK-125A1-1* Numerical Control lathe machine	*30HGSA* steel
TB, mushroom-headed screw, roll loading, horizontal stabilizer panels		*D16* duralumin
Variable EAPS	*EOSINT M270* laser sintering machine	*Direct Metall 2* powder sintered material
Engines package, FT with increased capacity, *KO-50* kerosene-combustion heater	*Zprinter 650 3D*-Printer	*ZP 150* powder composite material of black color
EAPS of *PAL* pyramid type, H-shaped HS with vertical fins, FT with increased capacity	*Viper si2TM* laser stereo lithography processing machine	*Accura ® 60 Plastic* liquid photopolymer [**)]

[*)] manufactured by "KATION" Company [10] at production site in Klin town, co-produced with "ANION", LLC (Limited liability company), (Russia) and "*Nylacast*"(Great Britain)

[**)] manufactured by *3D Systems Corporation* American Company [12].

a) CPF+TB+LG+NPF1+TPF1+TRP1+FT1+HS1+EAPS1 b) CPF+TB+LG+NPF2+TPF3+TRP1+FT3+HS3+EAPS1

c) CPF+TB+LG+NPF1+TPF1+TRP1+FT1+HS1+EAPS2 d) CPF+TB+LG+NPF3+TPF5+TRP2+FT2+HS2+EAPS1

Fig. 6. Variants of configuration of the variable wind-tunnel model of *Mil-171A2* helicopter

During tests the helicopter model is installed in the wind tunnel by using the two-panel suspension of the *6KT-1* aerodynamic balance (Fig. 7). This suspension consists of the system of load bearing wires (rods), which connect the model with the elements of the *6KT-1* aerodynamic balance, stiff supports and counterbalance weights. The *6KT-1* aerodynamic balance operates together with the measuring and computing complex. Such simultaneous work allows to control the experimental procedure according to the predefined plan, process the test data "at the speed of the experiment" and record the measurement results into computer memory as an ordered set of *.txt*- files.

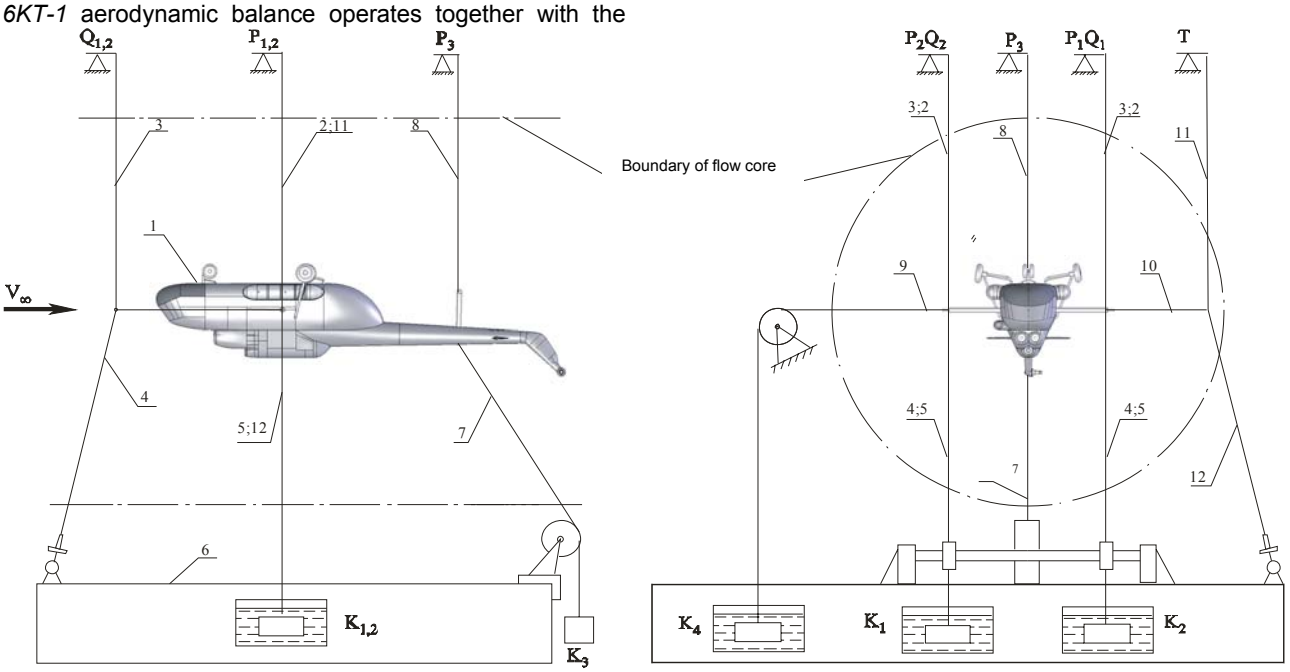

a) during the tests at various angles of attack;

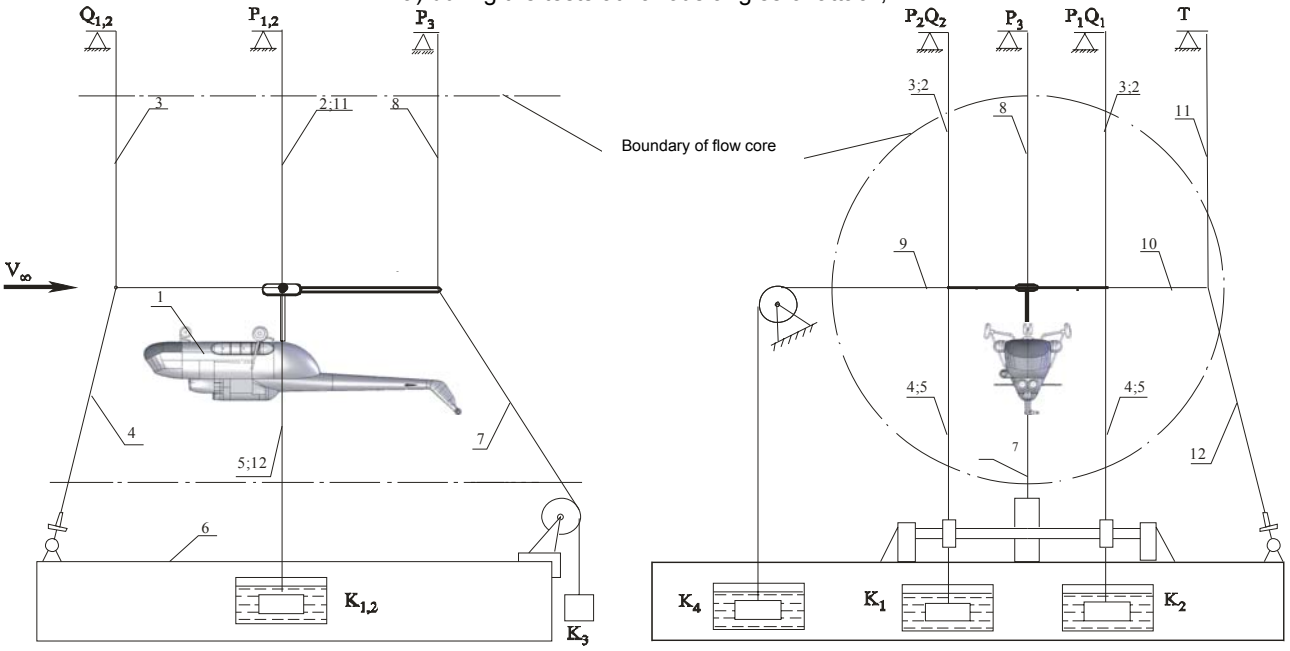

b) during the tests at various yaw angles

Fig. 7. Chart of installation of the variable wind-tunnel model of *Mil*-171A2 helicopter on the two-panel suspension of the *6KT-1* aerodynamic balance

1 – model, 2- rods $P_{1,2}$, 3 – vertical rods $Q_{1,2}$, 4 – inclined rods $Q_{1,2}$, 5 – counterbalance weight rods $K_{1,2}$, 6 - aerodynamic balance platform, 7 - counterbalance weight rod K_3, 8 – rod P_3, 9 - counterbalance weight rod K_4, 10 – horizontal rod T, 11 – vertical rod T, 12 - inclined rod T

The 6KT-1 aerodynamic balance is equipped with three groups of measurement facilities. These facilities are intended for measuring the three forces that act on the model: the Y_a lift force, the Q drag force, the T side force. The M_x, M_y and M_z moments are calculated based on the data of measurements of the components of Y_a, Q and T forces. The Y_a lift force is resolved into three components (P_1, P_2, P_3), which are measured by the appropriate sensors. The M_x and M_z moments are calculated by processing the information from these sensors. The Q

drag force is resolved into two components (Q_1 and Q_2), which are measured by the appropriate sensors. The M_y moment is determined based on the data of measurement of the Q_1, Q_2 and T forces. Thus the following data is obtained from the aerodynamic balance sensors after the wind-tunnel model tests: P_1, P_2, P_3, Q_1, Q_2, T and zero reference points P_{10}, P_{20}, P_{30}, Q_{10}, Q_{20}, T_0.

The numerical values of the aerodynamic forces are calculated according to the following formulas

$$X_a = K_{Cx}\left[(Q_1 - Q_{10}) + (Q_2 - Q_{20})\right],\ Z_a = K_{Cz}(T - T_0),$$

$$Y_a = K_{P_{1,2}}\left[(P_1 - P_{10}) + (P_2 - P_{20})\right] + \kappa(P_3 - P_{30}),$$

$$M_x = K_{P_{1,2}}\left[(P_2 - P_{20}) - (P_2 - P_{20})\right],$$

$$M_y = K_{My}\left[(Q_2 - Q_{20}) - (Q_1 - Q_{10})\right],\ M_z = \kappa(P_3 - P_{30}),$$

where K_{Cx}, $K_{P_{1,2}}$, κ, K_{My}, K_{Cz} are the appropriate calibration constants of the sensors, which connect the signals from the sensors with the values of the measured forces.

Difficulties with fastening the wind-tunnel models to the suspension of the aerodynamic balance emerge during the tests of aircraft models, the main body configuration of which is a fin-stabilized body of rotation or close to such shape. This is connected with the following situation: it is impossible to mount the conventional forward stings with the required lateral base on the suspension because of the small transversal size of this suspension. Therefore such models are attached by a wire suspension with a round rod, which is fully fixed in a model body (Fig. 8a). It is necessary to note that the round rod changes the flow and slightly distorts the true pattern of model flow. The model should be taken off the sting and the tests of the suspension with the stings should be performed to obtain the aerodynamic characteristics of the suspension.

A special sting was designed to perform the model tests for a wide range of the yaw angles. This special sting consists of the following: a shaft; a rod; a saber; an external rotary unit, which provides the variation of the yaw angle β; an internal rotary unit, which provides the variation of the angle of attack α (Fig. 8b). Since the β-variation mechanism of the *T-1* wind-tunnel of MAI provides the variation of the yaw angle β within the range of $0° \le \beta \le 40°$, it is possible to divide the range of the yaw angle under study $-90° \le \beta \le 90°$ into following six sub-ranges: 1) $-100° \le \beta \le 60°$, 2) $-70° \le \beta \le -30°$, 3) $-40° \le \beta \le 0°$, 4) $-10° \le \beta \le 30°$, 5) $20° \le \beta \le 60°$, 6) $50° \le \beta \le 90°$. The transition from one sub-range to another is carried out via rotation of the shaft with the model onto β_y angle around the longitudinal axis of the sting. In this case, the angle-of-attack control is performed via rotation of the model onto α_y angle around the shaft. The range of the values of the angle-of-attack is constrained by $-24° \le \alpha \le 30°$.

a) on the round rod

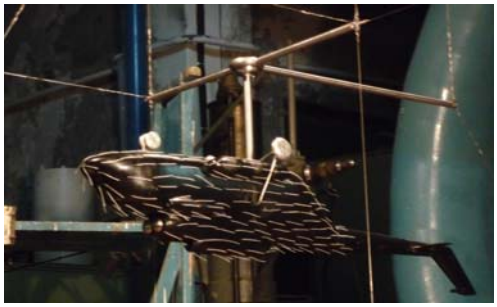

b) on the special sting

Fig. 8. The variants of the model suspension in the wind-tunnel

The test results are processed according to the following formulas:

a) in the wind-axis coordinate system

$$C_{\begin{pmatrix}x\\y\\z\end{pmatrix}a} = \frac{1}{q_{тр}S}\begin{pmatrix}X\\Y\\Z\end{pmatrix}_a,\ m_{\begin{pmatrix}x\\y\\z\end{pmatrix}a} = \frac{1}{q_{тр}Sl}M_{\begin{pmatrix}x\\y\\z\end{pmatrix}a},$$

where X_a, Y_a, Z_a - are the drag force, the lift force and the side force, which are measured by the aerodynamic balance;

M_{xa}, M_{ya}, M_{za} - are the rolling moment, the yawing moment and the pitching moment, which are derived from the experiment;

C_{xa}, C_{ya}, C_{za} - are the drag coefficient, the lift coefficient and the side-force coefficient;

m_{xa}, m_{ya}, m_{za} - are the rolling moment coefficient, the yawing moment coefficient and the pitching moment coefficient;

b) in the body-axis coordinate system

$$C_{\begin{pmatrix}x\\y\\z\end{pmatrix}} = \frac{1}{q_{тр}S}\begin{pmatrix}X\\Y\\Z\end{pmatrix},\ m_{\begin{pmatrix}x\\y\\z\end{pmatrix}} = \frac{1}{q_{тр}Sl}M_{\begin{pmatrix}x\\y\\z\end{pmatrix}}$$

where X, Y, Z - are the axial force, the normal force and the lateral force, which are measured by the aerodynamic balance;

M_x, M_y, M_z - are the rolling moment, the yawing moment and the pitching moment, which are derived from the experiment;

C_x, C_y, C_z - are the axial force coefficient, the normal force coefficient and the lateral force coefficient;

m_x, m_y, m_z - are the rolling moment coefficient, the yawing moment coefficient and the pitching moment coefficient;

S, l - are the reference area and the linear dimension of the model rotor with the radius of R = 0,5325 m;

$q_{тр}$ - is the dynamic pressure of the flow in the wind-tunnel $q_{wt} = 0{,}5\rho V_{wt}^2$.

The rolling moment coefficient, the yawing moment coefficient and the pitching moment coefficient are calculated about the model mass center (center of gravity).

The positive directions of the forces and moments, which act on the model, are shown in Fig. 9.

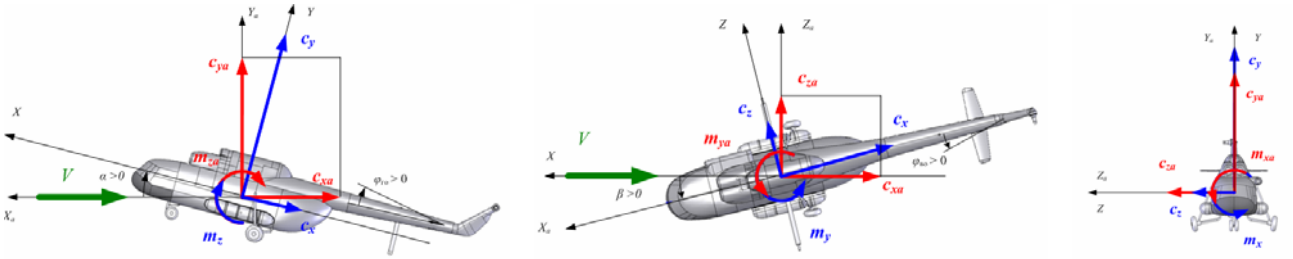

Fig. 9. The positive directions of the forces and moments, which act on the model

The processed results of the experiment contain a large amount of information, which can be represented in homogeneous table format. Therefore a computer program on the basis of *MS Excel* electronic spreadsheet was developed. This computer program transforms the table data from an arbitrary number of *.txt*-files into the set of diagrams, which contain families of one-parameter function curves.

The computer program is designed to perform the following operations:

1) selection of location and assignment of names of *.txt*-files with aerodynamic characteristics of the model, which are recorded in the wind-axis and body-axis coordinate systems;

2) assignment of argument name and number of test points along the argument axis,

3) assignment of parameter name, number of parameters and their notation conventions,

4) automatic input of information from the selected *.txt*-files into *.xls*-file and creation of the tables with the parameter and function values on the basis of this information. The created tables contain the aerodynamic characteristics of the model in the wind-axis and body-axis coordinate systems,

5) automatic plotting of the diagrams of model aerodynamic characteristics (families of curves) versus a given independent variable, which is plotted along the horizontal axis of the diagram, for a selected number of parameters.

Let us consider the examples of the three fundamental types of functions of model aerodynamic characteristics, which were studied in this paper.

The dependencies of model aerodynamic characteristics on the air flow velocity fall into the first category. The angle of attack α, the yaw angle β and the variable elements of the model can act as parameters for these dependencies. Fig.10 shows the results of the tests of the model configuration variant, which corresponds to the serially produced *Mil-17* helicopter configuration. These results are shown as diagrams of dependencies of the aerodynamic characteristics c_{xa}, c_{ya}, m_{za} on the air flow velocity V in the wind-axis coordinate system for the angles of attack α = *-20°, 0°, 20°* and the yaw angle β = *0*.

The tests were performed for the different values of the flow velocity in the wind-tunnel. This wind-tunnel flow velocity was varied within the range from *V = 10 m/sec* to V_{max} *= 45 m/sec*. The maximum flow velocity within the range is equivalent to the following values of the Reynolds number for the model (L_{mod}*= 0.95 m,* ν *= 1.45×10*$^{-5}$ *sec/m*^{2})

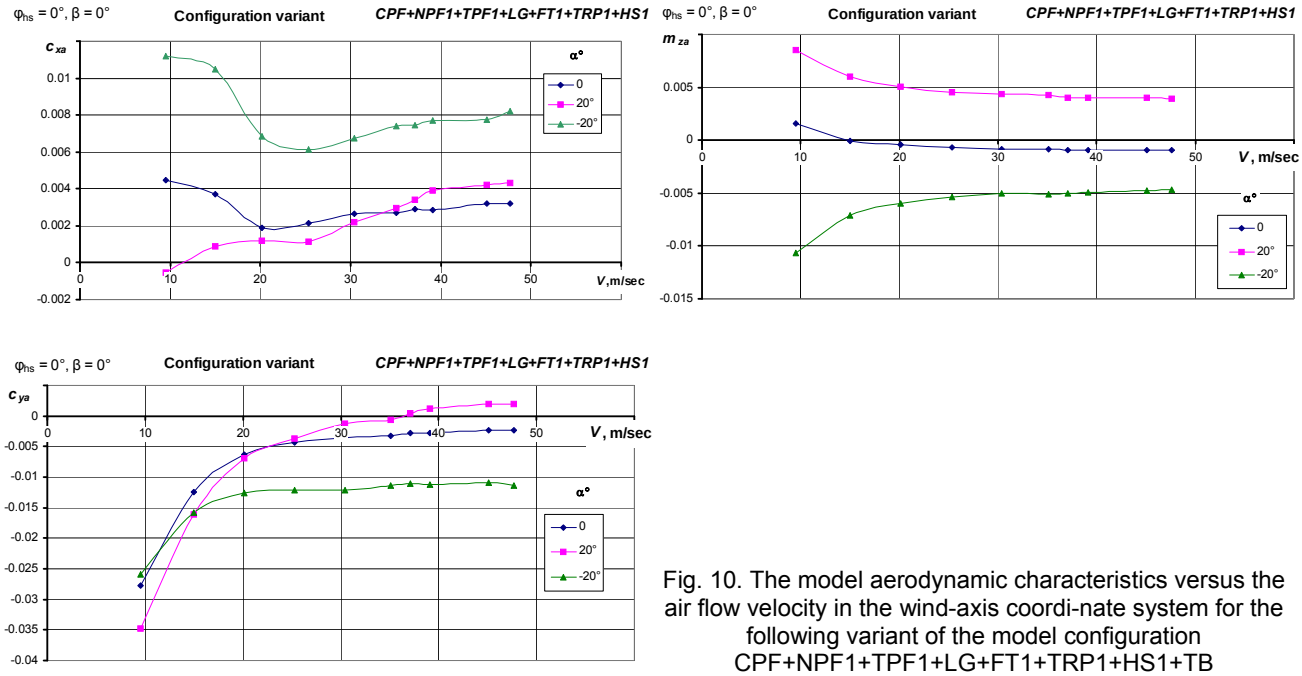

Fig. 10. The model aerodynamic characteristics versus the air flow velocity in the wind-axis coordi-nate system for the following variant of the model configuration CPF+NPF1+TPF1+LG+FT1+TRP1+HS1+TB

$$\mathrm{Re}_{\mathrm{mod}\max} = \frac{V_{\max} \times L_{\mathrm{mod}}}{\nu} = \frac{45 \times 0.95}{1.45 \times 10^{-5}} = 2.95 \times 10^{6}$$

The analysis shows that the self-similar flow mode emerges in the studied range of the angle of attack from the flow velocity of $V \approx 40$ *m/sec* for all aerodynamic characteristics of the model.

The dependencies of model aerodynamic characteristics on the angle of attack α fall into the second category. The parameters of these functions may include the following: yaw angle β, setting angle of the horizontal stabilizer φ_{hs} and the variable model elements (NPF, TPF, FT, HS, TRP, LG). Fig.11 shows the resulting data of the tests of the following variant of the model configuration: CPF+LG+NPF2+TPF3+TRP1+FT3+HS2+EAPS1. These results are presented as the diagrams of the aerodynamic characteristics c_{xa}, c_{ya}, c_{za}, m_{za} versus the angles of attack α in the wind-axis coordinate system. Here the setting angle of horizontal stabilizer φ_{hs} is used as a varied parameter to construct the families of curves.

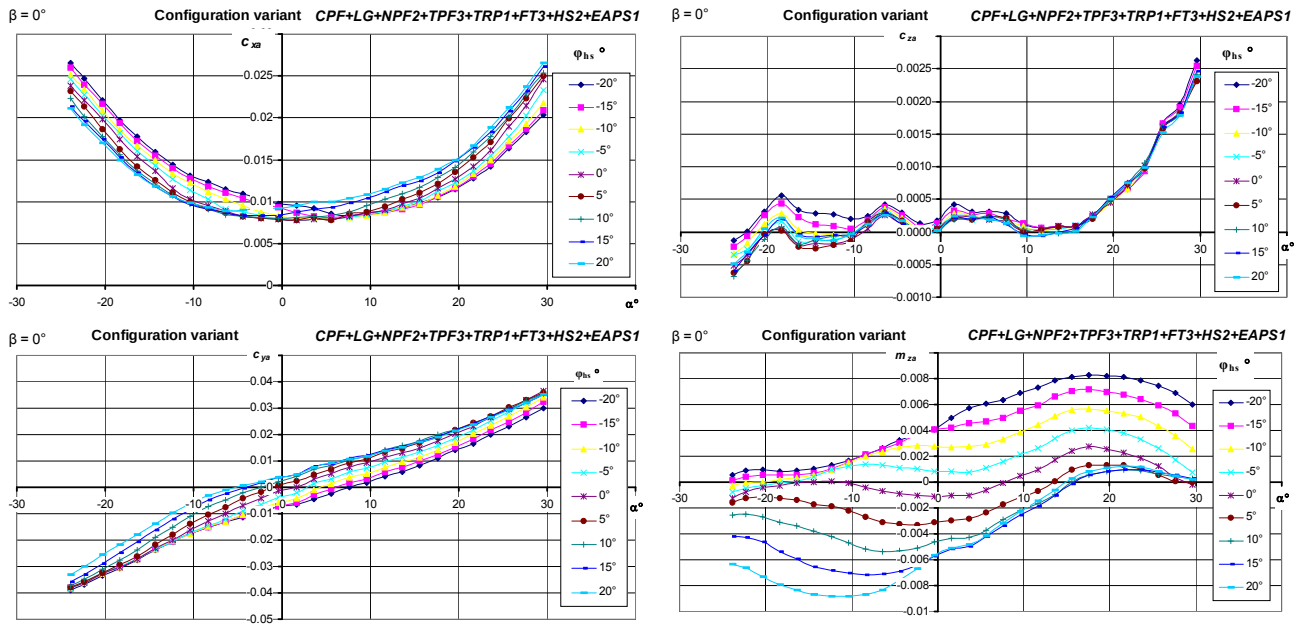

Fig. 11. The diagrams of the aerodynamic characteristics versus the angle of attack □ in the wind-axis coordinate system for the following variant of the model configuration: CPF+LG+NPF2+TPF3+TB+TRP1+FT3+HS2+EAPS1. The setting angle of horizontal stabilizer φ_{hs} is used as a varied parameter

The dependencies of model aerodynamic characteristics on the yaw angle β fall into the third category. The parameters of these functions may include the following: the angle of attack α, the setting angle of the vertical fin φ_{vf} and the variable model elements (NPF, TPF, FT, HS, TRP, LG). Fig.12 shows the resulting data of the tests of the following variant of the model configuration: CPF+LG+NPF2+TPF3+TRP2+FT2+HS1+EAPS1. These results are presented as the diagrams of the model aerodynamic characteristics c_{xa}, c_{za}, m_{xa}, m_{za} versus the yaw angles β in the wind-axis coordinate system. Here the setting angle of the vertical fin φ_{vf} is used as a varied parameter to construct the families of curves.

During the execution of the research the special attention was paid to confirmation of the reliability of the obtained results. Confirming reliability was important because the aerodynamic shape of the *Mil-171A2* helicopter model has a number of specific features. The qualitative influence of these specific features on the aerodynamic characteristics of the model was not known in advance. Another cause for paying special attention to results reliability validation consists in the subtlety of the differences between several variable airframe elements of the helicopter model (in the fact that the differences between some variable airframe elements of the helicopter model are not substantial enough). Therefore the following criteria were selected for confirmation of the testing results reliability:

1) the repeatability of the results of the tests of the same variant of the model configuration, which were obtained periodically (after a certain period of time);
2) the coincidence of the aerodynamic characteristics during the direct and reversed order of variations of angles of attack and yaw of the model for the same model configuration;
3) the coincidence of the aerodynamic characteristics for the same yaw angles, when the same variant of the model configuration is tested in “head up” and “head down” positions;
4) the coincidence rate of the model aerodynamic characteristics with the known experiment data, which was obtained by other authors under the same conditions.

The results of the series of the five identical tests of the variant of model configuration, which corresponds to the configuration of the serially produced *Mil-17* helicopter (CPF+NPF1+TPF1+TRP1+FT1+HS1+ EAPS1), with variation of the angle of attack showed that the aerodynamic characteristics $c_{xa}(\alpha)$, $c_{ya}(\alpha)$, $c_{za}(\alpha)$, $m_{za}(\alpha)$ repeat very well (their values coincide very well for all tests in the series). The values of the functions of the yawing moment coefficient $m_{ya}(\alpha)$ coincide a little bit worse. The maximum deviation of $m_{ya}(\alpha)$ values reaches up to $\Delta m_{ya} = 0.0002$. In this case the relative error in percent is equal to $\varepsilon_{my} = \Delta m_{ya} / m_{ya\,max} = 3.2\%$.

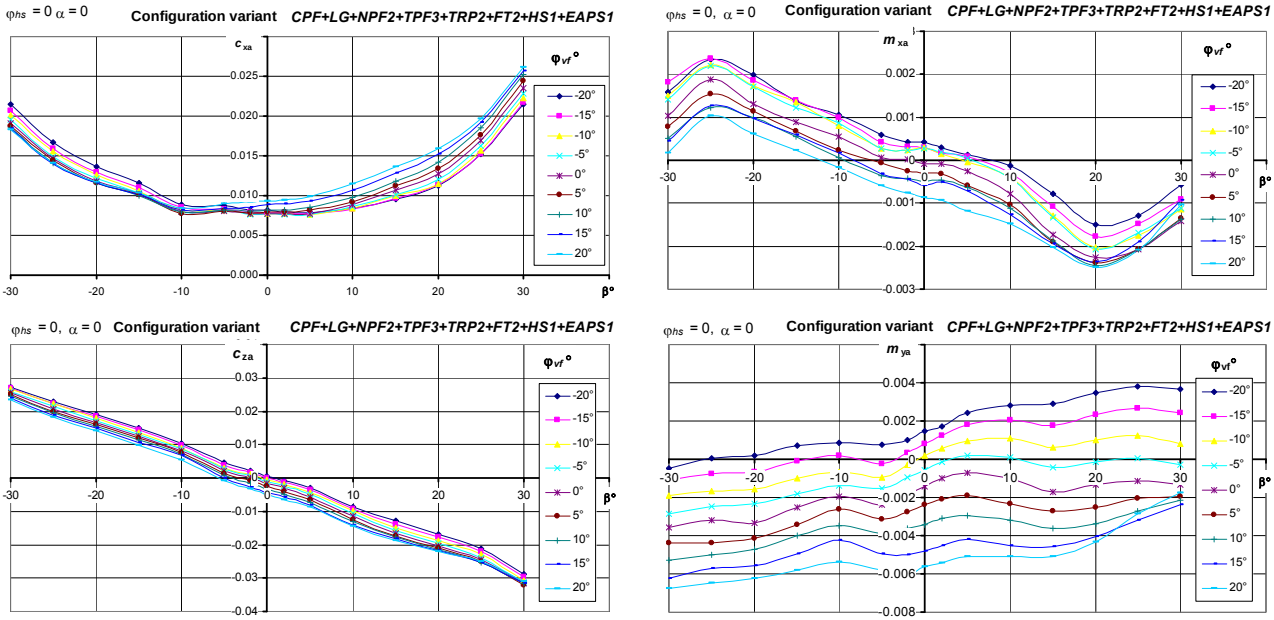

Fig. 12. The diagrams of the aerodynamic characteristics versus the yaw angle β in the wind-axis coordinate system for the following variant of the model configuration CPF+LG+NPF2+TPF3+TB+TRP2+FT2+HS1+EAPS1. The setting angle of the vertical fin φ_{vf} is used as a varied parameter

The good coincidence of the $c_{xa}(\alpha)$, $c_{ya}(\alpha)$, $c_{za}(\alpha)$, $m_{za}(\alpha)$ aerodynamic characteristics was obtained for the direct and reversed test process order. There are slightly bigger deviations for the values of the functions of the rolling moment coefficient $m_{xa}(\alpha)$ and the yawing moment coefficient $m_{ya}(\alpha)$. The small magnitude order of absolute values of the rolling moment and the yawing moment at the angle of yaw $\beta = 0$ (such situation is typical for helicopters) could be one of the possible reasons for such increase of deviations. The fact that the identical values of the aerodynamic characteristics were obtained for the same yaw angles for the "head up" and "head down" positions of the model can serve as one of the proofs of the experiment validity. The case is that the mechanism of variation of the yaw angle β in the *T-1 MAI* wind-tunnel works in only one direction and provides the values of the yaw angle β in the range from 2° to 35°. Therefore the tests, which were performed to obtain aerodynamic characteristics for the values of the yaw angle β that lie in the range from -30° to 30°, were carried out in two stages. First stage of tests was carried out for "head down" and second one for "head up" positions of the model. In the "head down" position the model was tested for the values of yaw angle β that lie within the range from -2° to 30° (Fig. 13a). In the "head up" position the model was tested for the values of yaw angle β that lie within the range from 2° to -30° (Fig. 13b). Such procedure allowed obtaining two functions, which share a common range of the values of the yaw angle $-2° \le \beta \le 2°$.

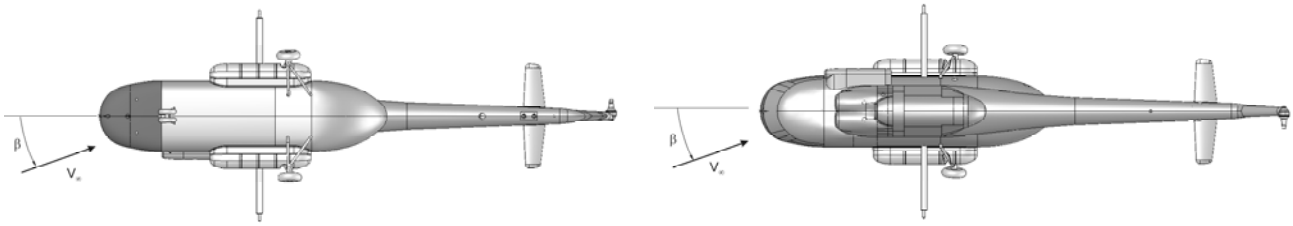

a) the "head down" position, the values of the yaw angle β are within the range from -2° to 30°

b) the "head up" position, the values of the yaw angle β are within the range from 2° to -30°

Fig. 13. The model position in the wind-tunnel

Fig. 14 presents the comparison results in the wind-axis coordinate system for the following configuration variant: CPF+NPF1+TPF1+TRP1+FT1+HS1+EAPS1.

It is possible to see that both branches of the curves that represent the dependencies of the force and moment coefficients on angles of attack coincide in the overlap zone ($-5° \le \beta \le 5°$). Such coincidence can be observed for the whole studied range of the values of angle of attack ($\alpha = -10°, 0°, 10°$).

It is usually assumed that the proximity of the shape of the function, which is built on the basis of the test results, to the known experiment data is the most objective sign of the reliability of these test results. In such verification the known experiment data should have been previously obtained during the tests of the similar model in other wind-tunnels under the similar conditions. Some information about the aerodynamic characteristics $c_x(\alpha)$, $c_y(\alpha)$, $m_z(\alpha)$ and $c_z(\beta)$, $m_x(\beta)$, $m_y(\alpha)$ of the *Mil-8* helicopter is available in public sources, However, this data is presented without any information about the configuration of the particular tested helicopter versions and modifications, which could have been implemented in these versions compared to serially produced version of the helicopter. The lack of this information complicates carrying out a correct comparison substantially.

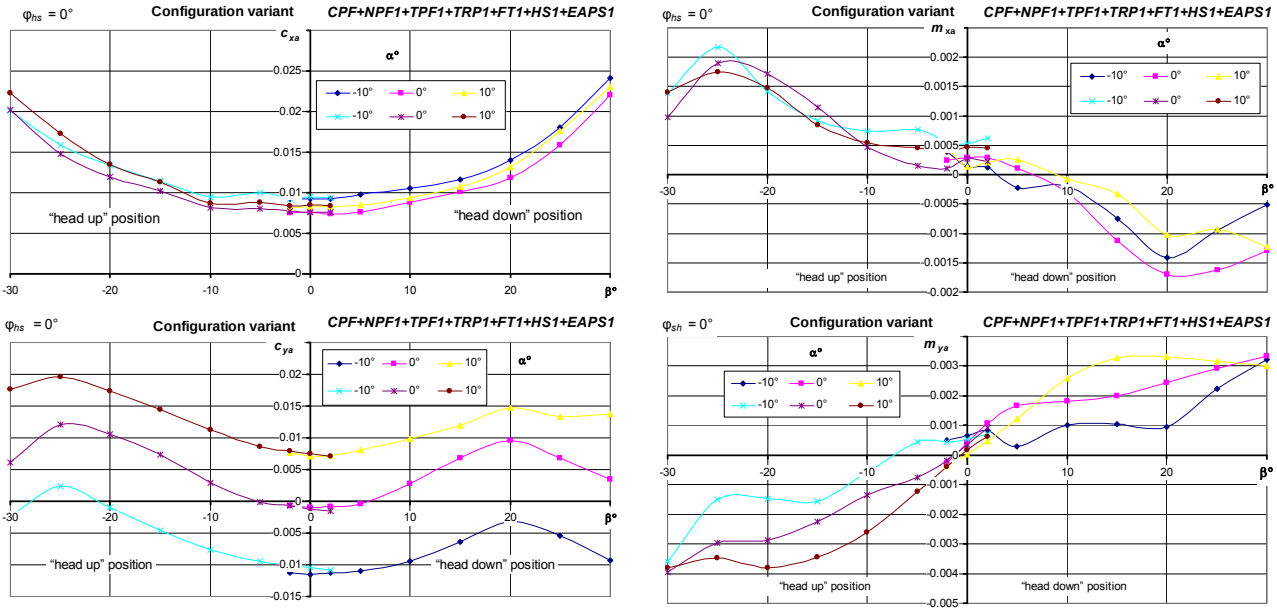

Fig. 14. The dependencies of the coefficients of aerodynamic forces and moments on the yaw angle in the wind-axis coordinate system for the "head up" and "head down" positions of the following variant of the model configuration CPF+NPF1+TPF1+TRP1+FT1+HS1+EAPS1

It is usually assumed that the proximity of the shape of the function, which is built on the basis of the test results, to the known experiment data is the most objective sign of the reliability of these test results. In such verification the known experiment data should have been previously obtained during the tests of the similar model in other wind-tunnels under the similar conditions. Some information about the aerodynamic characteristics $c_x(\alpha)$, $c_y(\alpha)$, $m_z(\alpha)$ and $c_z(\beta)$, $m_x(\beta)$, $m_y(\alpha)$ of the *Mil-8* helicopter is available in public sources, However, this data is presented without any information about the configuration of the particular tested helicopter versions and modifications, which could have been implemented in these versions compared to serially produced version of the helicopter. The lack of this information complicates carrying out a correct comparison substantially.

It is known from [3, 5, 14] that the first prototype version of *V-8* helicopter was equipped with one engine and two short external fuel tanks of the same size, which were located on both sides of the fuselage (1961). After that, the second prototype version of the helicopter was created (1962). It was equipped with two engines and designated as *V-8A*. The serially produced versions of this helicopter were designated as *Mil-8P* (passenger version) and *Mil-8T* (transport or cargo version). The aerodynamic drag of one of these versions was reduced. Besides, these helicopters were manufactured with two versions of fuel tanks: the long version with the capacity of 1154 (left) and 1044 (right) liters; the short version with the capacity of 680 (left) and 745 (right) liters.

The analysis of the published pictures of the versions of *Mil-8* helicopter shows that the right fuel tank of the *Mil-8P* helicopter version (1965) was "lengthened" by mounting the fairing of the *KO-50* kerosene-combustion heater in its forward part [3]. The preliminary project of the *Mil-8M* helicopter version with the lengthened fuselage was developed in 1971. Afterwards this version was designated as *Mil-8MT* or *Mil-17*. In 1977 during the second stage of modernization process the fuselage of Mil-8MT helicopter was lengthened by 0.5 meters on both sides relative to the centre of gravity. After that this version was designated as *Mil-18*. In 1984 the aerodynamic configuration of the *Mil-18* helicopter was changed substantially due to mounting the fuel tanks under the cabin floor, changing the tail part of fuselage and introducing landing-gear retraction. All these improvements decreased the aerodynamic drag of the helicopter considerably. Thus there were, at least, five different variants of fuselage. Strictly speaking, the dependencies of aerodynamic characteristics of these fuselage variants on the angle of attack and the yaw angle should differ from each other.

At first it is necessary to analyze the functions of aerodynamic drag coefficient of *Mil-8* helicopter airframe without the external fuel tanks. These functions were obtained in the wind-tunnel of TsAGI [8] for the different variants of the helicopter model. Fig. 15a shows the diagrams of these functions designated by diamond markers (without landing gear) and square markers (with main and forward landing gear legs). The aerodynamic shapes of the fuselage and fuel tanks of the tested model were not specified in the referenced source [8]. Fig. 15a also shows the diagrams of $c_{xa}(\alpha)$ functions designated by solid lines (without the tail rotor pylon) and dashed lines (with the tail rotor pylon). These diagrams of $c_{xa}(\alpha)$ functions were obtained from the results of our tests for the variants of the model with landing gear (pink color) and without landing gear (blue color). It is necessary to point out that the aerodynamic characteristics shown at the Fig. 15 were calculated by using the area of the fuselage mid-section as the characteristic area. The fuselage mid-section area of the MAI model was equal to $S_{fms} = 0.0202$ m^2. It is possible to see that the aerodynamic drag of the model, which was created at TsAGI, at the angle of attack $\alpha = 0$ is slightly less than that of the model, which was created at MAI. This situation can be explained by the higher Reynolds numbers, which were achieved during the process of tests at TsAGI. The analysis of the results of

the tests of the TsAGI and MAI models without landing gear shows that their $c_{xa}(\alpha)$ functions are closer to each other for the negative values of the angle of attack. The analysis of the results of the tests of the TsAGI and MAI models with landing gear shows that their $c_{xa}(\alpha)$ functions are closer to each other for the positive values of the angle of attack.

Monograph [1] provides a limited set of diagrams of aerodynamic characteristics of the *Mil-8* helicopter, which includes the following functions: $m_{za}(\alpha)$, $c_{za}(\beta)$, $m_{ya}(\beta)$, $m_{xa}(\beta)$. All of these functions were obtained from the tests in the TsAGI wind-tunnel. However, the monograph [1] does not give information about the configuration of the tested model. Therefore further comparison of the results of the tests, which were carried out at MAI, would be made by using the base variant of the wind-tunnel model. This base variant of the model corresponds to *Mil-171A2* helicopter and has the following configuration: CPF+NPF1+TPF1+TRP1+FT1+HS1+EAPS1.

It is necessary to mention that the aerodynamic characteristics, which are presented in these diagrams, were calculated by using the mentioned above area of the fuselage mid-section as the characteristic area. It is also important to note that the fuselage length was used as the characteristic dimension for the calculations. The fuselage length of the tested model was equal to $L_m = 0.95$ *m*.

Fig. 15b shows the functions of the pitching moment coefficient of the *Mil-8* helicopter airframe, which were obtained at TsAGI. These function values were acquired for different variants of the model configuration: for the variant with fuel tanks (designated by diamond markers) and for the variant without fuel tanks (designated by square markers). Fig. 15b also shows the $m_{za}(\alpha)$ diagrams, which were obtained from the results of our tests for the variants of the model with fuel tanks (blue color) and without fuel tanks (pink color). The results of tests of the model without fuel tanks are shown for two variants: with landing gear (designated by solid line) and without landing gear (designated by dashed line). The comparison shows that the qualitative character of the functions, which were obtained from both tests (at MAI and at TsAGI), is absolutely identical. However, the derivatives $dm_z/d\alpha$ of the TsAGI test functions are slightly smaller than those of the MAI test functions. The quantitative agreement of the results of both tests (at MAI and at TsAGI) is wholly satisfactory for the positive values of the angle of attack, i.e. the difference between the results does not exceed 3%. The difference between the test results for the negative values of the angle of attack is bigger, but it does not exceed 28%. It is not possible to explain this 28% mismatch, because there is no opportunity (not enough information) to compare the configuration shapes of these two models (MAI and TsAGI).

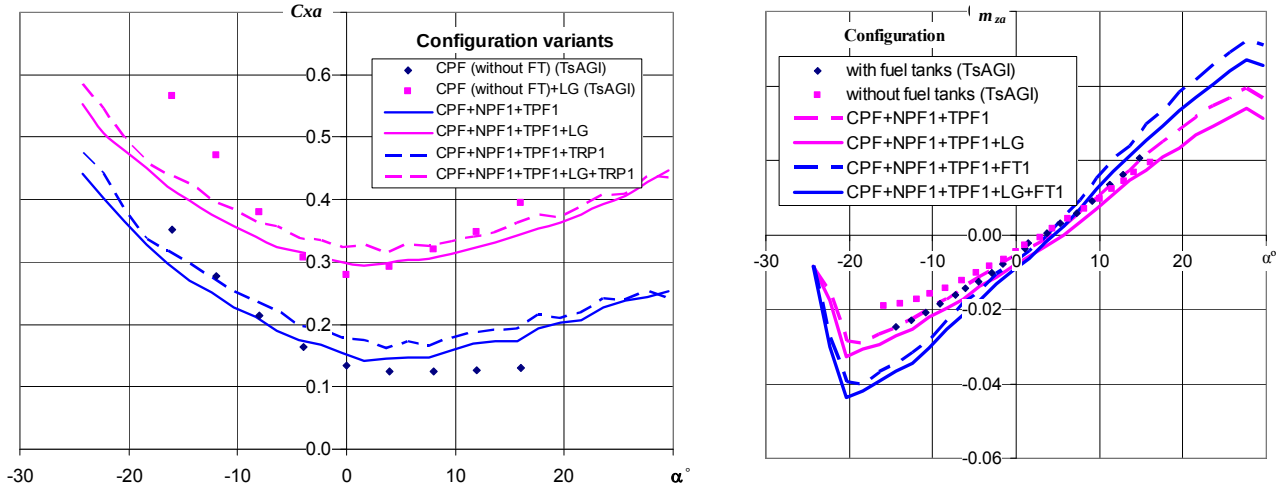

a) the functions of the aerodynamic drag coefficient versus the angle of attack $c_{xa}(\alpha)$

b) the functions of the pitching moment coefficient versus the angle of attack $m_{za}(\alpha)$

Fig. 15. The comparison of the aerodynamic characteristics of the *Mil-171A2* helicopter model with the TsAGI test results [1, 8]

Let us now discuss the materials, which are adduced in the technical manual of *Mil-8* helicopter [2]. We can compare the airframe aerodynamic characteristics, which this technical manual contains, with the aerodynamic characteristics of the two following variants of the *Mil-171A2* helicopter model: CPF+LG+NPF1+TPF1+TRP1+ +FT1+HS1 and CPF+LG+NPF1+TPF1+TRP1+FT1+HS1+ +EAPS1. The aerodynamic configurations of these two variants of the model are the nearest to that of the *Mil-8* helicopter.

Fig. 16 shows the functions of the drag coefficient $c_{xa}(\alpha)$ and lift coefficient $c_{ya}(\alpha)$ versus the angle of attack from the technical manual [2]. These functions are designated by markers. Fig. 16 also shows the diagrams of MAI test results for two variants of the model configuration: with horizontal stabilizer and without horizontal stabilizer. These results are designated by solid lines. It is possible to conclude from the diagrams at the Fig. 16 that the functions $c_{ya}(\alpha)$ from MAI test results and technical manual coincide very well for the variant with horizontal stabilizer at the setting angle $\varphi_{hs} = 0$. The test results function $c_{xa}(\alpha)$ of the variant of MAI model with the horizontal stabilizer is closer to the function from the technical manual [2] at the high angles of attack. The deviation is equal to $\Delta c_{xa} \approx 0.002$ (or 26.3%) when $\alpha = 0$. This can be caused by the difference between Reynolds numbers, which were achieved in the tests from the technical manual [2] and MAI tests, as well as certain difference between the shapes of the fuselage mid-sections.

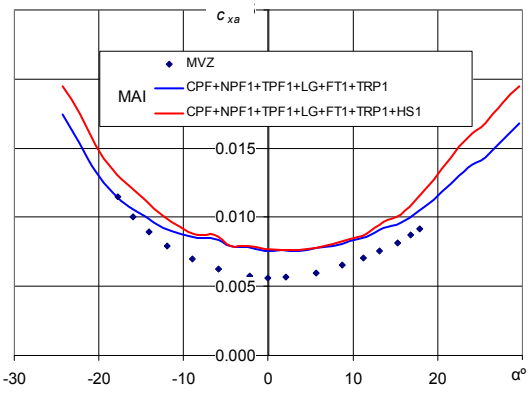

a) the function of the drag coefficient versus the angle of attack $c_{xa}(\alpha)$

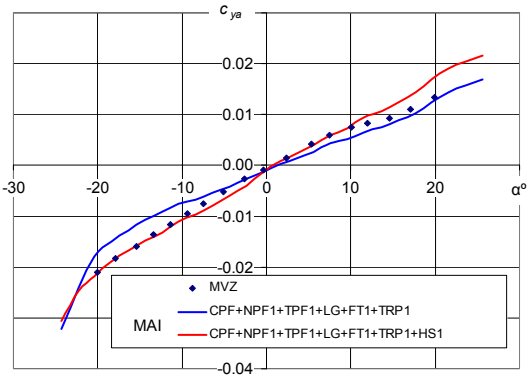

b) the function of the lift coefficient versus the angle of attack $c_{ya}(\alpha)$

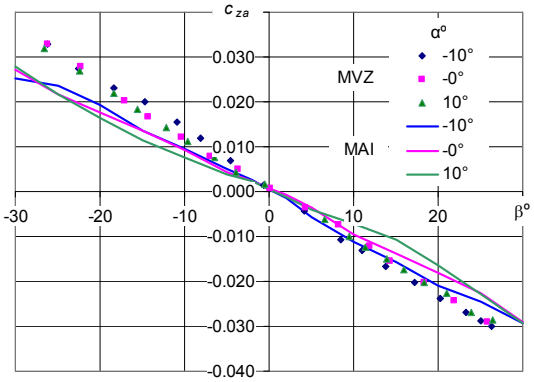

c) the functions of the side-force coefficient versus the yaw angle $c_{za}(\beta)$

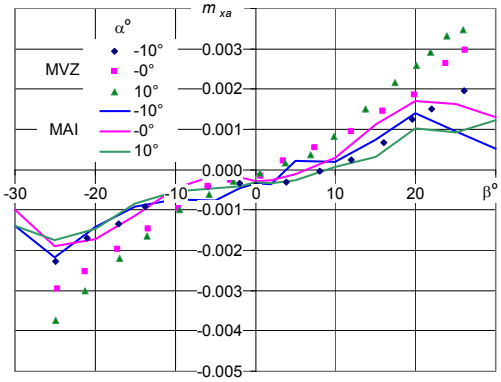

d) the functions of the rolling moment coefficient versus the yaw angle $m_x(\beta)$

Fig. 16. The aerodynamic characteristics of the *Mil-171A2* helicopter model against the data from the technical manual of the *Mil-8* helicopter

Fig. 17 confirms this assumption. It shows two identically scaled contours of the fuselage mid-sections: contour of the *Mil-8* helicopter mid-section, which was obtained from the drawing of its main view [2]; contour of the *Mil-171A2* helicopter mid-section, which was obtained from the *3D*-model of its surface. It is possible to see that the fuselage mid-section of the *Mil-171A2* helicopter is slightly bigger than that of the *Mil-8* helicopter. The values of the actual areas of the fuselage mid-sections will be the following: $S_{Mil\text{-}8} = 6.27\ m^2$ and $S_{Mil\text{-}1712A} = 6.5\ m^2$. This difference plays its role during the comparison of the aerodynamic characteristics, which are divided by the rotor disk area. In particular, it can result in the higher value of the airframe drag coefficient of the *Mil-171A2* helicopter. This phenomenon can be observed in the Fig. 16a.

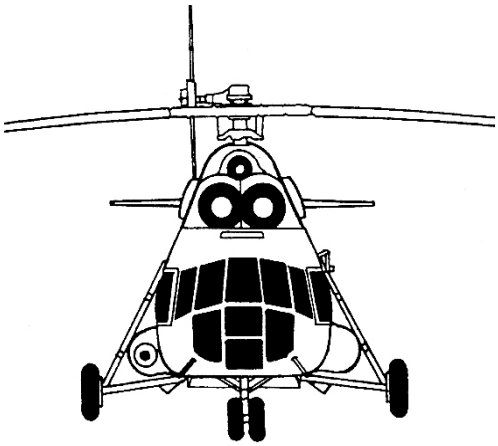

a) *Mil-8MT* helicopter

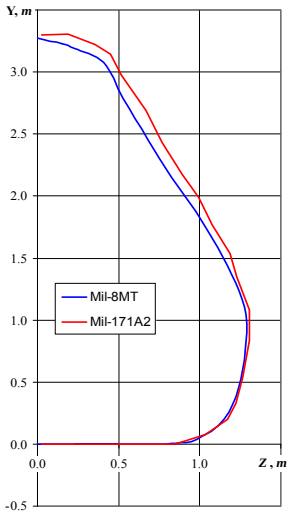

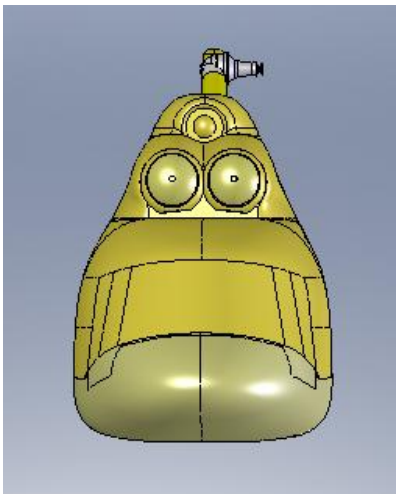

b) *Mil-171A2* helicopter

Fig. 17. The contours of the fuselage mid-sections of the *Mil-8MT* helicopter and the *Mil-171A2* helicopter

Conclusions

1. The modern technologies of the rapid three-dimensional prototyping allow for swift creation of the aircraft wind-tunnel models at an affordable cost. The shape of their surface can be sufficiently complex as the creation of these models is based on their *3-D* virtual models. The accuracy of manufacturing provides for the smooth transitions from one conjugated element of the model to another for all variants of the model configuration.
2. The conditions of the tests in *T-1* wind-tunnel of MAI, during which the aerodynamic characteristics of the *Mil-171A2* helicopter model were obtained, meet the requirements of self-similarity. During the test process the whole yaw angle range was segmented into two sub-ranges. The model was mounted in “head up” and “head down” positions for the tests in different sub-ranges of the yaw angle. This approach allowed obtaining the consistent aerodynamic characteristics in the overlap zone, which served as one of the signs of the reliability of the obtained test results.
3. In general the obtained results are in accordance with the results of the tests of the various models of the *Mil-8* helicopter, which were obtained in the TsAGI wind-tunnels previously. The longitudinal aerodynamic characteristics (C_{xa} ,C_{ya} , m_{za}) agree well with TsAGI results both for the various angles of attack and the yaw angles. The dependencies of the lateral aerodynamic characteristics (C_{za} ,m_{xa} , m_{ya}) on the values of the yaw angle agree with TsAGI results slightly worse.

References

1. Braverman A.S., Perlshtein D.M., Lapisova S.V. Single-Rotor Helicopter Trimming. Moscow, Mashinostroenie, 1975.
2. Mil-8 Helicopter. Technical Manual. Mashinostroenie, 1970.
3. Danilov V.A., Drugov A.G., Teterin I.V. Mil-8 Helicopter. Moscow, Transport, 1979.
4. Dmitriev V.G., Bun’kov N.G., Vermel’ V.D. Generation of External Aircraft Geometry on a Computer at the Stage of Scientific Research, Computer-Aided Design and Computer-Aided Manufacturing of the Aerodynamic Models. In the Collected Book: “Russian Encyclopedia of CALS. Aero-Space Machine Engineering”. Under the editorship of A.G. Bratukhin. – Moscow, NITs ASK, 2008.
5. Mikheev V.R. Moscow Helicopter Plant n.a. M.L. Mil. Moscow, Polygon Press, 2007.
6. Panchenko V.Ya. (ed.) Laser Technologies of Materials Processing: Modern Problems of Fundamental Research and Applied Developments. Section “Laser Technology of Rapid Prototyping and Direct Fabrication of Three-Dimensional Objects”. – Moscow: Fizmatlit, 2009. – 664 pp.
7. Sirotkin O.S., Tarasov Yu.M., Rytsev S.B., Girsh R.I. Prototyping and Technology of Layer-by-Layer Synthesis in the Modern Computer-Aided Manufacturing. In the Collected Book: “Russian Encyclopedia of CALS. Aero-Space Machine Engineering”. Under the editorship of A.G. Bratukhin. – Moscow, NITs ASK, 2008.
8. Tarasov N.N. Experimental Research of Aerodynamics of Helicopter Airframes and Tail Rotors. Proceedings of the 1st Forum of Russian Helicopter Society. vol. 1. Moscow, 20-21 September 1994.
9. http://ru.wikipedia.org/wiki/%D0%9C%D0%B8-171
10. http://www.kation_msk.ru/ru/products/catalog/cast_nylon
11.http://www.oboronprom.ru/catalog/helicopters/modernizirovannyi-srednii-vertolet-mi-171a2
12.http://production3dprinters.com/materials/accura-60-plastic
13.http://www2.uuaz.ru/news/news/news20120123_1.htm
14. Mikheyev V.R. Mi-8: 40 years and still going strong. Polygon-Press, 2001.